

Adjustable refractive power from diffractive moiré elements

Stefan Bernet* and Monika Ritsch-Marte

Division for Biomedical Physics, Innsbruck Medical University, A-6020 Innsbruck, Austria

*Corresponding author: Stefan.Bernet@i-med.ac.at

Received 28 April 2008; revised 12 June 2008; accepted 13 June 2008;
posted 19 June 2008 (Doc. ID 95463); published 11 July 2008

We show how suitable combinations of cascaded diffractive optical elements (DOEs) can form a combined “moiré DOE” of adjustable refractive power and high diffraction efficiency. The optical power can be adjusted continuously by a mutual rotation of one DOE with respect to the other. Fresnel lenses and axicons of variable refractive power or spiral phase plates of adjustable helical charge can be realized this way. © 2008 Optical Society of America

OCIS codes: 050.1970, 120.4120, 220.4298.

1. Introduction

Diffractive optical elements (DOEs) are optical components consisting of microscopic phase structures in a transparent material [1]. Commercially available DOEs include lenses, arrays of lenses, or holograms (so-called kinoforms [2]) that project specified patterns, such as lines, crosshairs, or dot arrays. Each pixel of a DOE shifts the phase of an incident light beam within an interval between 0 and 2π . The transmitted wave then carries the predesigned wavefront modulation.

There exist many algorithms (e.g., kinoform algorithm, Gerchberg–Saxton algorithm [3], etc.) to calculate the DOEs dedicated to perform the desired tasks. In the production process of a DOE, the corresponding phase landscapes are imprinted into a material with techniques such as photolithography, electron beam lithography, or mechanical micromachining (diamond turning), such that each spot of the material delays the phase of an incoming light beam by the desired phase value. This can be achieved with either a modulated surface profile (which is, for example, etched into a quartz plate) or by a spatially modulated index of refraction as in, for example, a photopolymer film.

An important difference of computer-generated DOEs, compared to normal holograms that are recorded by superposition of an object and a reference wave, is the fact that DOE phase structures are typically not harmonic; i.e., they locally correspond to blazed gratings with a sawtooth phase profile. As a result, the diffraction efficiency of a properly designed DOE can reach 100%, in contrast to the 40% achieved by normal phase holograms with harmonic grating structures.

The transmission function $T(x,y)$ of a DOE is a “phase-only landscape” of the form $T(x,y) = \exp[i\Phi(x,y)]$, where $\Phi(x,y)$ is an array of pixels in a range between 0 and 2π , corresponding to the phase shift a light beam acquires when passing through the corresponding spot. If two DOEs with transmission functions $T_1(x,y) = \exp[i\Phi_1(x,y)]$ and $T_2(x,y) = \exp[i\Phi_2(x,y)]$ are placed directly behind each other, then the transmission function T_{joint} of the combined DOE becomes

$$\begin{aligned} T_{\text{joint}}(x,y) &= T_1(x,y)T_2(x,y) \\ &= \exp\{i[\Phi_1(x,y) + \Phi_2(x,y)]\}. \end{aligned} \quad (1)$$

The principle of our suggested system is indicated in Fig. 1. Two DOEs are cascaded such that the resulting total transmission function can be changed continuously by a simple mutual rotation of the two DOEs. The underlying principle is similar to

0003-6935/08/213722-09\$15.00/0
© 2008 Optical Society of America

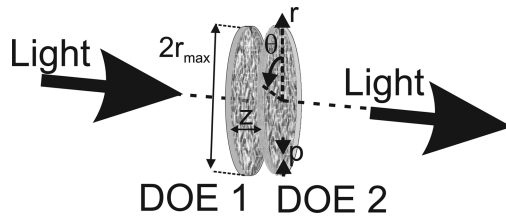


Fig. 1. Generic setup (not to scale): two diffractive optical elements (DOEs) are placed directly behind each other. They can be mutually rotated around a central axis. This combined optical element manipulates the wavefront of an incident light wave in a predefined way that changes with the mutual rotation angle.

the well-known moiré effect, where a combination of two gratings with similar grating constants yields a structure with a much larger spatial beating period. Typically the moiré effect is generated with absorptive rather than phase structures, and the transmission function consists of locally harmonic (i.e., symmetric, nonblazed) gratings, resulting in a total diffraction efficiency that is low (<6%).

It has already been described in the literature how to calculate fringe patterns to obtain varifocal Fresnel lenses, with a focal length that can be changed by a lateral shift of one element with respect to the other [4,5] or by a mutual rotation [6]. However, a significant disadvantage in this case is the fact that the overall diffraction efficiency is rather small, first because the moiré elements are absorptive and, second, because the fringe patterns are harmonic; i.e., they diffract a large part of the illumination light into undesired diffraction orders. It has also been known for a long time [7] that a theoretical efficiency of 100% is possible with a pair of DOEs consisting of blazed phase structures. Later, the principle was generalized to DOEs that produce various effects, for instance, a change in refractive power upon general geometric transformations, such as translation, resizing, or rotation of one of the DOEs with respect to the other [8].

In this work we perform a systematic investigation of combined DOE elements that are rotated with respect to each other. This comprises varifocal Fresnel lenses, axicons of adjustable refractive power, or spiral phase plates of variable helical charge. Such rotationally variable elements are of practical interest because they do not change the effective aperture and because a mutual rotation is easy to implement in an optical setup.

It turns out that the periodicity of the rotation imposes some restrictions on the performance of the combined moiré diffractive optical elements (MDOEs) that were not mentioned in earlier work. The problem is that a rotation by an angle θ in one direction corresponds to a rotation of $2\pi - \theta$ in the other direction. This introduces an ambiguity into the features of the MDOE. For example, if a MDOE is designed to produce an adjustable Fresnel lens, it actually generates *two* different lenses in adjacent sectors of the MDOE. We describe how such a sector formation can be avoided by a modification of the phase profile structures. In this case, the MDOE can, at least in a

limited range of rotation angle, be used as an efficient optical element.

2. Basic Principle

An interesting class of MDOEs that have almost 100% diffraction efficiency [7,8] consists of two DOEs with a complex conjugate transmission function, i.e.,

$$\begin{aligned} T_1(r, \varphi) &= \exp[i\Phi(r, \varphi)], \\ T_2(r, \varphi) &= \exp[-i\Phi(r, \varphi)]. \end{aligned} \quad (2)$$

To facilitate the description of the mutual rotation, polar coordinates r and φ are introduced, where the radial coordinate r is measured from the center of the DOE. If the second DOE (T_2) is rotated by an angle θ , then the joint (total) transmission function becomes

$$T_{\text{joint}}(r, \varphi; \theta) = \exp\{i[\Phi(r, \varphi) - \Phi(r, \varphi - \theta)]\}. \quad (3)$$

The exponent can be expanded in a Taylor series in θ :

$$T_{\text{joint}}(r, \varphi; \theta) = \exp\left\{i\left[\frac{\partial\Phi(r, \varphi)}{\partial\varphi}\theta - \frac{1}{2}\frac{\partial^2\Phi(r, \varphi)}{\partial\varphi^2}\theta^2 + \dots\right]\right\}. \quad (4)$$

If we consider only phase functions Φ that can be factorized into a r -dependent and a φ -dependent contribution, i.e., $\Phi(r, \varphi) = \Phi_r(r)\Phi_\varphi(\varphi)$, then Eq. (4) becomes

$$T_{\text{joint}}(r, \varphi; \theta) = \exp\left\{i\Phi_r(r)\left[\frac{d\Phi_\varphi(\varphi)}{d\varphi}\theta - \frac{1}{2}\frac{d^2\Phi_\varphi(\varphi)}{d\varphi^2}\theta^2 + \dots\right]\right\}. \quad (5)$$

If one further sets $\Phi_\varphi(\varphi) = \varphi$, the Taylor series terminates after the first term

$$T_{\text{joint}}(r, \varphi; \theta) = \exp\{i\Phi_r(r)\theta\}. \quad (6)$$

This suggests that one can generate any freely selectable radial profile Φ_r , i.e., any profile that depends only on r , but not on φ , with a variable scaling factor proportional to θ . Since θ can be continuously adjusted in an interval $[0, 2\pi]$ by rotating one DOE with respect to the other, the scaling of the r -dependent phase function Φ_r is continuously adjustable. Important examples for radially symmetric phase functions are Fresnel lenses, axicons, or combinations of these, which will be further discussed in the following.

For practical purposes it is advantageous that all DOEs that have the property

$$\Phi(r, \varphi) = -\Phi(r, -\varphi) \quad (7)$$

produce their corresponding complex conjugate when reversed, since this operation replaces the coordinates (r, φ) by $(r, -\varphi)$. In these cases one can take a pair of identical DOEs, turn one of them upside down and place it face-to-face on top of the other in

order to get the desired MDOE element. Note that this condition is fulfilled for the above-mentioned class of radially symmetric MDOEs, where $\Phi_\varphi(\varphi) = \varphi$, with arbitrarily selectable Φ_r dependence.

3. Varifocal Fresnel Lens

The transmission function of a lens with focal length f , or refraction power f^{-1} , for a wavelength λ is given by $T_{\text{lens}} = \exp(-i\pi r^2/\lambda f)$. If the corresponding parabolic phase profile is taken modulo- (2π) , it corresponds to a Fresnel lens, or to a so-called “kinoform” of a lens [2]. Comparing this with Eq. (5) and (6), it turns out that such a parabolic phase profile can be obtained by setting $\Phi_\varphi(\varphi) = \varphi$ and $\Phi_r(r) = ar^2$ with a freely selectable constant a , which will be shown later to be a linear scaling factor for the optical power of the combined DOE system.

In this case, the transmission functions become

$$\begin{aligned} T_1 &= \exp[iar^2\varphi], \\ T_2 &= \exp[-iar^2\varphi]. \end{aligned} \quad (8)$$

To produce phase plates that correspond to these transmission functions, the complex angles (i.e., the arguments of the exp function) have to be taken modulo- (2π) such that the result consists of an array of phase values in $[0, 2\pi]$. The corresponding phase patterns of the two DOEs are plotted in Fig. 2.

There (and in all further DOE plots), gray values between white and dark correspond to phase values in the range $[0, 2\pi]$. The two transmission functions T_1 and T_2 are complex conjugates. Since they satisfy the symmetry condition of Eq. (7), the two DOEs are reversed images of each other. Thus, for practical purposes, two identical DOEs with the same transmission function T_1 , which are positioned face-to-face, can be used.

If the second DOE, T_2 , is rotated by a certain angle θ , then the total transmission function of the MDOE element becomes

$$T_{\text{joint}} = \exp[iar^2\varphi] \exp[-iar^2(\varphi - \theta)] = \exp[ia\theta r^2]. \quad (9)$$

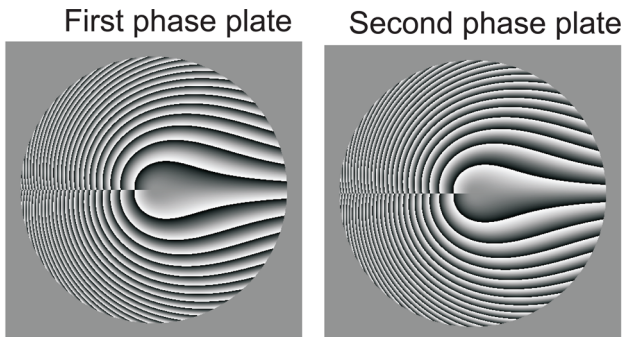


Fig. 2. A MDOE that acts as a Fresnel lens with a refractive power that depends on their mutual rotation angle. Gray values in the figure actually correspond to phase-shift values between 0 and 2π . Note that the two DOEs are identical if one of them is reversed (i.e., flipped upside down).

As mentioned before, such a transmission function corresponds to that of an ideal lens with a refractive power f^{-1} of

$$f^{-1} = a\theta\lambda/\pi. \quad (10)$$

Therefore, the change of the optical power depends linearly on the mutual rotation angle θ , i.e., $df^{-1}/d\theta = a\lambda/\pi$. The corresponding phase transmission function of the combined DOE system corresponds to a kinoform of an ideal lens that has, due to its asymmetric, sawtoothlike phase grating structure, almost 100% diffraction efficiency; i.e., such a DOE element acts for the designed light wavelength as a normal glass lens.

The corresponding phase patterns created by the MDOE system are plotted in Fig. 3 for some positive and negative rotation angles θ . The figure shows that the MDOE corresponds to a Fresnel lens with a variable (positive or negative) refractive power, depending on the rotational direction. The positive and negative refractive powers can be distinguished in the plots by the direction of the radial phase change.

However, there appears an effect that is not expected at first: in addition to the desired Fresnel lens, a sector appears that includes another Fresnel lens pattern with another focal length. This sector consists of the area between the two radial lines at $\varphi = \pi$ and $\varphi = \pi + \theta$. The reason for the appearance of these sectors is the periodicity of the function in Eq. (9), i.e., a clockwise angular rotation of $|\theta|$ is indistinguishable from a counterclockwise rotation by an angle of $-(2\pi - |\theta|)$. According to Eq. (10), the two cases correspond to two Fresnel lenses with different refractive powers of

$$f_1^{-1} = a|\theta|\lambda/\pi, \quad f_2^{-1} = -a(2\pi - |\theta|)\lambda/\pi, \quad (11)$$

respectively. Since the rotation angle $|\theta|$ can be adjusted in a range between 0 and 2π , the correspond-

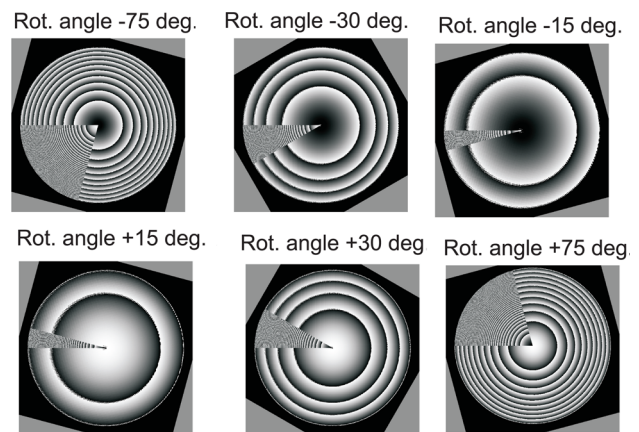


Fig. 3. Superposition of the two DOEs in Fig. 2 at different mutual rotation angles of (upper row) -75° , -30° , and -15° ; and (lower row) $+15^\circ$, $+30^\circ$, and $+70^\circ$. The results are perfect blazed Fresnel lenses with different refractive powers; however, they include a sector of an angular range that corresponds to the mutual rotation angle that comprises a Fresnel lens of a different focal length.

ing two focal lengths f_1 and f_2 have a different sign and a different absolute value.

This sectoring effect can be disturbing for imaging applications. One possible remedy is to cover the undesired sector by an absorbing mask but, fortunately, it is also possible to avoid the sectoring altogether with a modified phase profile, as will be shown below.

A. Varifocal Fresnel Lens Avoiding Sector Formation

Computer simulations show that the appearance of the undesired sector is due to the fact that the phase profile of the two DOEs (Eq. (8)) does not change continuously when following a circle around the origin. Instead, there are phase jumps which are not just integer multiples of 2π , and which appear along the radial line at the polar angle $\varphi = \pi$, e.g., at the lines from the center to the left edges the DOEs in Fig. 2. To avoid this discontinuity, the phase profile can be slightly modified to

$$\begin{aligned} T_1 &= \exp[i \text{round}\{ar^2\}\varphi], \\ T_2 &= \exp[-i \text{round}\{ar^2\}\varphi], \end{aligned} \quad (12)$$

where the $\text{round}\{\dots\}$ operation means rounding of the argument to the next higher integer number. An example for the corresponding phase patterns of the two DOEs is plotted in Fig. 4. The patterns look very similar to those of the first method (Fig. 2) and the two DOEs are still inversion symmetric, but the phase edges now appear rougher. On the other hand, the discontinuities at the radial line at the polar angle $\varphi = \pi$ have disappeared.

The transmission function of the rounded MDOE is plotted in Fig. 5 for the same rotation angles as in Fig. 3. Obviously, there is no sector formation anymore. The transition from negative to positive refractive powers upon changing the mutual rotation angle is smooth, forming a blazed Fresnel lens with a well-defined focal length for small mutual rotation angles (as shown in the range between -30° and $+30^\circ$ in Fig. 5). For larger rotation angles (e.g., 75°), the sawtooth grating passes over into a corresponding binary grating, which means that the efficiency of the combined Fresnel lens decreases and that the lens be-

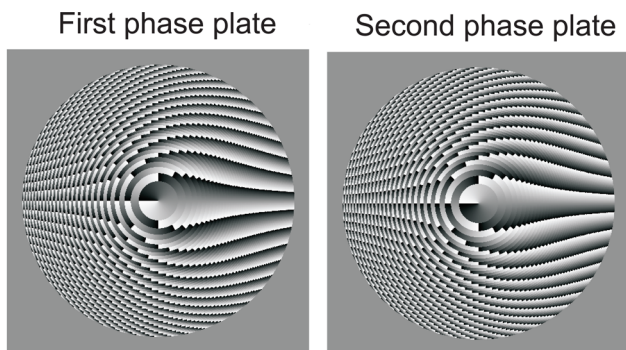


Fig. 4. MDOEs forming an adjustable Fresnel lens. The MDOE is similar to the one in Fig. 2; however, it is calculated according to Eq. (12) such that there are no phase discontinuities (with the exception of 2π phase jumps) along circular paths around the center.

comes bifocal; i.e., it has two different focal lengths simultaneously.

The reason for this behavior is again the intrinsic ambiguity of the rotation angle between an angular rotation of $|\theta|$ and $-(2\pi - |\theta|)$. Now the corresponding two Fresnel lenses of different refractive powers are not formed at different angular zones (i.e., in different sectors) of the MDOE (Fig. 3), but instead are embedded within one continuous phase structure. Again, the MDOE comprises two superposed Fresnel lenses with refractive powers of $f_1^{-1} = a\theta\lambda/\pi$ and $f_2^{-1} = -a(2\pi - |\theta|)\lambda/\pi$, respectively. The relative efficiency of the two lenses varies as a function of the mutual rotation angle; i.e., for small angles θ there is a major contribution of the lens term f_1 that passes over into a dominant lens term f_2 for angles larger than π .

Figure 6 sketches the diffraction efficiency of the two superposed lenses as a function of the mutual rotation angle in a range between -2π and $+2\pi$. The calculations are carried out in the Fresnel approximation by first multiplying the joint transmission function for each rotation angle θ with a parabolic phase factor $\exp(i\pi r^2/\lambda f_{1,2})$, where $f_{1,2}$ corresponds to the two focal lengths of the bifocal Fresnel lens according to Eq. (11). Then a numerical two-dimensional Fourier transform of the result is performed and the field in the center of the resulting two-dimensional array (i.e., in the focal spot) is read out.

The continuous curve corresponds to the diffraction efficiency of the first Fresnel lens term with focal length f_1 . It has its largest efficiency at a zero rotation angle (corresponding to a refractive power of 0), and it falls off only smoothly (by less than 15%) in an interval between -90° and $+90^\circ$. On the other hand, the efficiency of the second superposed Fresnel lens remains below 15% within this interval. There the refractive power of this second, undesired lens is very different from the first one; i.e., it is close to the maximal value of $f_2^{-1} = \pm 2a\lambda$, but of low efficiency. Note that at a zero rotation angle the refractive power of

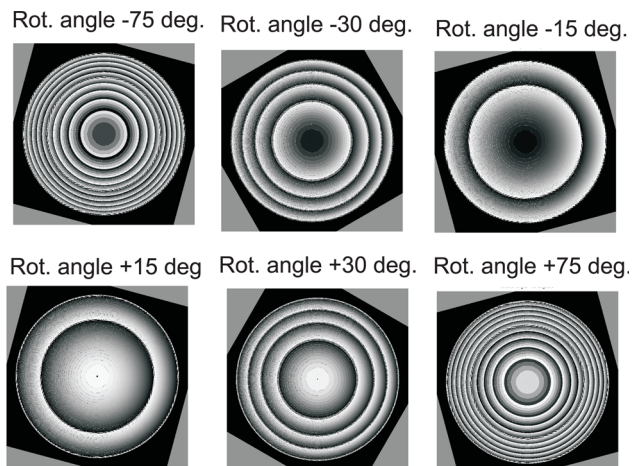


Fig. 5. Result of the superposition of the two DOEs of Fig. 4 at different mutual rotation angles of (upper row:) -75° , -30° , and -15° ; and (lower row:) $+15^\circ$, $+30^\circ$, and $+75^\circ$. A sector formation like that in Fig. 3 is now avoided.

the second lens jumps from $f_2^{-1} = +2a\lambda$ to $f_2^{-1} = -2a\lambda$, but at this angular position the efficiency of the corresponding lens in fact vanishes, such that the jump does not appear as a physically observable discontinuity. It is also interesting that this efficiency dependence on the rotation angle is different from that of the “simple” Fresnel MDOEs that are calculated according to Eq. (8). There, the efficiency of the two superposed lenses just changes linearly between 0 and 100% with the rotation angle; i.e., there the efficiency ratio is just determined by ratio of the sector areas in which the two different Fresnel lenses are displayed. The nonlinear (cosinlike) dependence obtained for the Fresnel MDOEs with avoided sector formation in Fig. 6 has the advantage that a change of the refractive power around its minimal value produces only a second-order change in the corresponding efficiency.

If one of the two DOEs is continuously rotated with constant speed with respect to the other, the corresponding Fresnel lens is periodically scanning within an adjustable range of focal lengths. This may have applications in imaging systems (inspection cameras) and beam scanning systems.

B. Practical Considerations

The maximally adjustable focal range for $\theta \in (-2\pi, 2\pi)$ is given in Eq. (10), i.e., $f^{-1} = a\theta\lambda/\pi$. There is, however, a limitation on the maximal value of the constant a that is imposed by the resolution of the physical DOE. To resolve a grating that is printed as a pixel array, the maximal phase shift between two adjacent pixels has to be smaller than π , i.e.

$$\frac{d\Phi}{dr} < \frac{\pi}{p} \quad \text{and} \quad \frac{d\Phi}{rd\varphi} < \frac{\pi}{p}, \quad (13)$$

where p is the size of one DOE pixel. The first and second conditions determine the radial and tangential

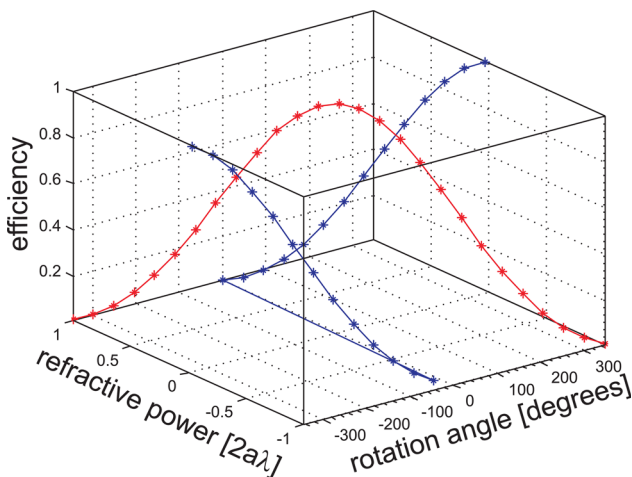


Fig. 6. (Color online) Diffraction efficiency and refractive power of the Fresnel lenses in Fig. 5 as a function of the mutual rotation angle between the two DOEs. The joint DOE corresponds to a bifocal Fresnel lens with two refractive powers (red and blue curves), the relative efficiencies of which depend on the rotation angle.

phase resolution, respectively. For DOEs generating Fresnel lenses it turns out that the first condition is always more restrictive than the second one [9], thus, in the following it can be considered alone.

Since the DOEs have the transmission functions $T_{1,2} = \exp[\pm iar^2\varphi]$, one has $\Phi = \pm iar^2\varphi$. Together with Eq. (13), this yields the condition

$$2ar_{\max}\varphi_{\max} < \pi/p, \quad (14)$$

where r_{\max} is the maximal radius of the DOE and φ_{\max} is the maximal polar angle. Since φ is limited to a range between $-\pi$ and π , φ_{\max} corresponds to π , and the condition becomes

$$a < 1/2pr_{\max}, \quad \text{i.e., } a_{\max} = (1/2pr_{\max}). \quad (15)$$

Thus, the maximal a value for a certain DOE depends on both its pixel resolution and the desired maximal radius.

According to Eq. (10), the refraction power of the MDOE lens with such a a_{\max} value is $f^{-1} = a_{\max}\theta\lambda/\pi$. In the previous section, it was shown that for getting an efficiency of $>85\%$, the rotational range of θ should be limited to an interval between $-\pi/2$ and $+\pi/2$. Thus, by inserting $\theta = \pm\pi/2$ altogether, one derives the limitation

$$-f_{\min}^{-1} < f^{-1} < +f_{\min}^{-1}, \quad (16)$$

where

$$f_{\min} = 4pr_{\max}/\lambda \quad (17)$$

is the smallest focal length of the MDOE that still has a diffraction efficiency of over 85%, and which is actually achieved at a mutual rotational angle of $\pi/2$. As a practical example, a DOE with a typical pixel size of $p = 1 \mu\text{m}$ and a diameter of $2r_{\max} = 10 \text{ mm}$ has a refraction power adjustable in a range between -25 and $+25$ diopters (corresponding to a focal length range between $\pm 4 \text{ cm}$ and $\pm\infty$) at a wavelength of 500 nm .

A further point of practical importance is the robustness of the method against misalignment, which may arise if the two adjacent DOEs are not centered perfectly. At first glance, it might be assumed that such a misaligned pair loses its intended function. Figure 7 shows a simulation for the joint transmission function of two misaligned DOE types (left two columns: Fresnel lens MDOE according to Eq. (8); right two columns: Fresnel lens with avoided sector formation according to Eq. (12)). The MDOEs are simulated for two different mutual rotation angles of 10° and 30° . From the top to the lowest row, the simulated misalignment (i.e., the decentering of the rotation axis from the DOE center) changes from 1 pixel to 5 and 10 pixels. Since the MDOEs have a size of $512 \text{ pixels} \times 512 \text{ pixels}$, this corresponds to a mutual decentering of 0.2%, 1%, and 2% of the two DOEs with respect to their diameter.

Our simulations show that such a misalignment leads to lens errors, such as astigmatism, and the originally spherical Fresnel lens becomes elongated in

the direction of the lateral displacement. The relative lens error (as compared to the curvature of the lens) seems to become smaller for larger rotation angles, which indicates that the lens deformation stays constant, whereas the refractive power increases with increasing rotation angle. Further simulations of the point spread function of the distorted lenses (not presented here) indicate that they do not lose their functionality of focusing light near the precalculated focal plane. The simulations show a smooth gradual dependence of the introduced lens errors on the misalignment; i.e., for small decentering there is no abrupt failure of the MDOE performance. Thus, a pixel-by-pixel transverse alignment is a desirable, but not an indispensable, prerequisite.

There exists a physical restriction for the maximally allowed axial distance between the two DOEs. To assure that the light diffracted from one pixel of the first DOE passes through the correct pixel of the second DOE, the distance between the two DOEs should be at least a factor of 2 smaller than the Talbot length $L_{\text{Talbot}} = 2p^2/\lambda$, since at this distance a grating replicates with a π -shifted phase. According to this criterion (at a wavelength of $\lambda = 500$ nm), the axial distance between two DOEs with a pixel size of $p = 1 \mu\text{m}$ should be smaller than $2 \mu\text{m}$, whereas a larger pixel size of $4 \mu\text{m}$ allows for an axial distance of approximately $32 \mu\text{m}$. Concerning the robustness of method with respect to lateral displacements, it may be expected that also a larger axial distance will not automatically lead to an abrupt functionality loss of the element.

C. Advantageous Modifications

In many cases, it is not desired to change the refraction power of a lens symmetrically around zero

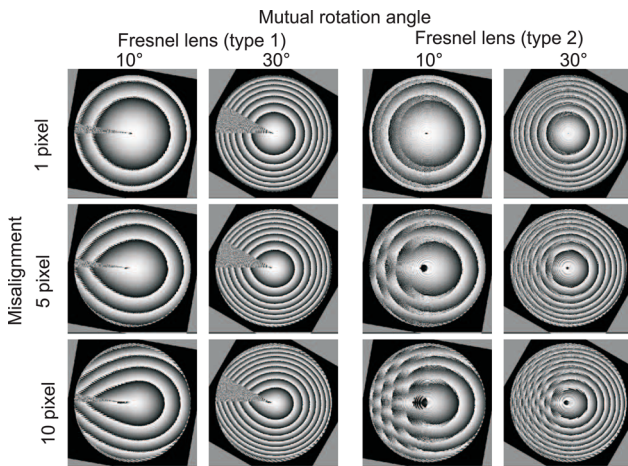


Fig. 7. Sensitivity of MDOEs to transverse misalignment: MDOEs generating a Fresnel lens (left two columns), and a Fresnel lens with avoided sector formation (right two columns), are plotted for two mutual rotation angles of 10° and 30° , and for three different decentering values of 1 pixel (upper row), 5 pixels (middle row), and 10 pixels (lowest row). The total size of each MDOE is $512 \text{ pixels} \times 512 \text{ pixels}$. The misalignment introduces lens deformations but it does not completely destroy the performance of the element.

power, but instead around a certain offset value. This might be achieved by placing the combined DOE element directly behind a “normal” glass lens that acts as an offset. However, this can be also achieved without an external glass lens, by multiplying the transmission functions of each of the two DOEs with an offset lens term, each supplied with half of the required refraction power f_{offset}^{-1} , i.e.,

$$\begin{aligned} T_1 &= \exp[i \text{round}\{ar^2\}\varphi] \exp(i\pi r^2/2f_{\text{offset}}\lambda), \\ T_2 &= \exp[-i \text{round}\{ar^2\}\varphi] \exp(i\pi r^2/2f_{\text{offset}}\lambda). \end{aligned} \quad (18)$$

In this case, the MDOE changes its focal length as a function of the mutual rotation angle as before (see Fig. 6), but now around an offset focal length, f_{offset} . The balanced distribution of the offset factor among the transmission functions has the advantage that they still fulfill the symmetry condition of Eq. (7), such that an upside-down flip of one DOE generates the other. An example of two DOEs according to Eq. (18) is shown in Fig. 8.

4. Axicons with Variable Refraction Power

The above considerations can be generalized to produce all kinds of MDOE elements for any radially symmetric phase transmission function. One important member of this class is an axicon, defined by its transmission function $T_{\text{axicon}} = \exp(iar)$. Such axicons produce so-called Bessel beams, which are circularly symmetric beams with an axially elongated focal region, which are applied, for example, in laser cutting systems, optical tweezers, or for fiber coupling. In analogy with the construction of the Fresnel lens, an axicon is obtained by setting $\Phi_\varphi(\varphi) = \varphi$ and $\Phi_r(r) = ar$, where a is again a constant that can be chosen.

The transmission functions of the two DOEs generating an axicon become

$$\begin{aligned} T_1 &= \exp[iar\varphi], \\ T_2 &= \exp[-iar\varphi]. \end{aligned} \quad (19)$$

An example for such a transmission function is plotted in Fig. 9(a). If such a DOE is rotated by an angle of 25° with respect to its (reversed) counterpart,

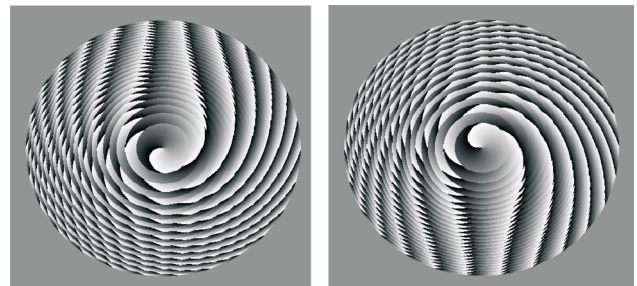


Fig. 8. Two DOEs calculated according to Eq. (18) produce a combined DOE acting as a varifocal Fresnel lens with an offset refraction power; i.e., at a zero mutual rotation angle, the focal length is f_{offset} .

the joint transmission function shown in Fig. 9(d) results. Similar to the last section, the refractive power of the axicon formed by the combination of these two DOEs is proportional to the constant a and to the mutual rotation angle θ .

Obviously, there is again the effect that an undesired sector forms that contains an axicon with a different refractive power. Similar to the last section, the formation of such a sector can be avoided by including a rounding operation, i.e.,

$$\begin{aligned} T_1 &= \exp[i \text{round}\{ar\}\varphi], \\ T_2 &= \exp[-i \text{round}\{ar\}\varphi]. \end{aligned} \quad (20)$$

An example for such a transmission function is plotted in Fig. 9(b) and the result of the MDOE for a mutual rotation angle of 25° is shown in Fig. 9(e). In analogy to the last section, the combined transmission function corresponds to that of two superposed axicons of different refractive powers. As before, the relative efficiency of the second axicon structure is again below 15%, as long as the mutual rotation angle is limited to the interval between -90° and $+90^\circ$.

Finally, it might be desirable to produce an axicon lens, i.e., an axicon with a variable refractive power that is superposed by a normal focusing or diverging Fresnel lens of a fixed focal power f_{offset} . The corresponding formula for getting such an element is

$$\begin{aligned} T_1 &= \exp[i \text{round}\{ar\}\varphi] \exp(i\pi r^2/2f_{\text{offset}}\lambda), \\ T_2 &= \exp[-i \text{round}\{ar\}\varphi] \exp(i\pi r^2/2f_{\text{offset}}\lambda), \end{aligned} \quad (21)$$

and an example for a corresponding MDOE is plotted in 9(c).

Such a structure can, for example, produce a ring-shaped light intensity distribution from an incoming plane light wave that focuses at a certain distance behind the element. Rotating one of the DOEs with respect to the other leads to a changing radius of the focused light ring. The DOE structure has the advantage that the desired axicon-shaped light field has a different divergence compared to residual nondiffracted light, which corresponds to the zero diffraction order of the combined DOE. Such residual light may appear if the DOE is not realized perfectly, e.g., if the calculated phase values are not properly reconstructed in the physical DOE structure. Because of the different divergences of the desired axiconlike diffracted light and the undesired nondiffracted light, the two components can easily be separated, as with an aperture stop directly in the focal plane of the zero-order light.

Another interesting transmission function which is radially symmetric and which can therefore be produced by the above mentioned method is that of a pure phase shifter, i.e., $T_{\text{shifter}} = \exp(ia\theta)$, where θ is again the mutual rotation angle. According to the above considerations, this can be produced by combining two DOEs with transmission functions of $T_{1,2} = \exp(\pm ia\varphi)$. Using such a MDOE as a phase

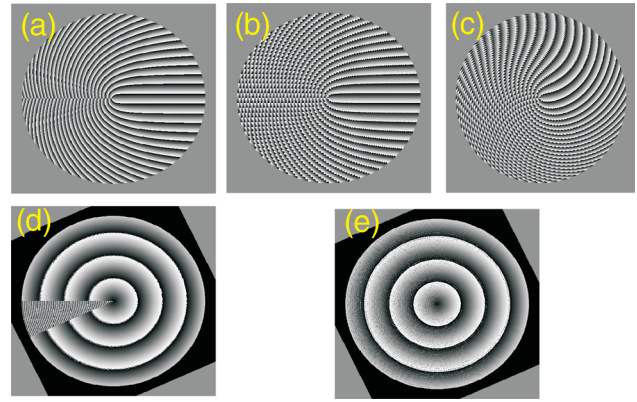


Fig. 9. Calculated DOEs for creating an axicon with a refractive power that depends on the mutual rotation angle. All DOEs in (a), (b), and (c) have to be combined with a second DOE that is identical to the first one, but flipped upside down. The DOE in (a) is calculated according to Eq. (19) and produces a perfect blazed axicon with, however, an undesired sector [see example (d)] for a mutual rotation angle of 25° . The DOE in (b) is calculated according to Eq. (20) and produces axicons without the undesired sector formation [see example (e)]. The DOE in (c) is calculated according to Eq. (21) and produces an axicon with a variable refractive power that is superposed by a Fresnel lens with a constant focal length.

shifter in interferometers has the advantage that the phase is changing continuously by just keeping up the rotation of one DOE with respect to the other. The integer constant a acts as a gear factor that translates rotational angles into phase shifts.

5. Spiral Phase Element with a Variable Helical Index

In the following, an example is investigated that is not radially symmetric and which, therefore, cannot be generated as before, i.e., by just setting $\Phi_\varphi(\varphi) = \varphi$ and $\Phi_r(r)$ to the desired r -dependent function. The desired transmission function is now given by $T_{\text{spiral}} = \exp(i\ell\varphi)$, which corresponds to a spiral phase plate [10,11] with a helical charge of ℓ .

Spiral phase elements have important applications in beam shaping for generating doughnut beams, which are used for optical trapping [12,13] in laser tweezers, for transferring angular momentum to microscopic particles [14,15], for digital spiral imaging [16], for spiral phase contrast imaging in microscopy [17,18] and interferometry [19], or for STED microscopy [20]. Here we design a set of two successive DOEs that can act as a spiral phase element with a continuously adjustable helical charge. The basic transmission functions of the corresponding DOEs are given by

$$\begin{aligned} T_1 &= \exp[ia\varphi^2], \\ T_2 &= \exp[-ia\varphi^2], \end{aligned} \quad (22)$$

where a is a constant that determines the change in the helical index of the combined DOE as a function of the rotation angle. An example for a set of DOEs with the transmission functions according to Eq. (22) is shown in Fig. 10. Note that now the symmetry

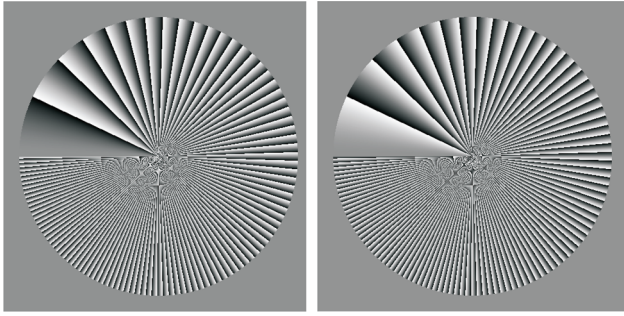


Fig. 10. Example for a set of DOEs that generates a spiral phase element with a variable helical index that depends linearly on the mutual rotation angle between the two DOEs.

condition of Eq. (7) is not satisfied anymore, which means that the two DOEs are not just mirror images of each other. Therefore, for this specific task two different DOEs have to be produced individually.

The transmission function of the combined DOE at a mutual rotation angle of θ now becomes

$$\begin{aligned} T_{\text{joint}} &= \exp(ia\varphi^2) \exp[-ia(\varphi - \theta)^2] \\ &= \exp(i2a\theta\varphi) \exp(-ia\theta^2). \end{aligned} \quad (23)$$

The first factor corresponds to the transmission function of a spiral phase plate with a helical index of $\ell = 2a\theta$ and the second factor to a spatially uniform phase shift by an amount of $-a\theta^2$. If such a combined DOE is used as a mode converter, the helicity of the joint spiral phase element can be linearly adjusted by the mutual rotation angle θ , whereas the associated uniform phase shift does not play a role. The transmission functions of the MDOE element are shown in Fig. 11 for various rotation angles.

Because of the mentioned phase ambiguity, the combined spiral phase element contains two helical indices of $\ell_1 = 2a\theta$ and $\ell_2 = -2a(2\pi - \theta)$ in two different sectors, respectively. Using $T_{1,2} = \exp[i \text{round}\{\alpha\varphi\}\varphi]$, in analogy to the modifications mentioned before, turns out to be less useful here than

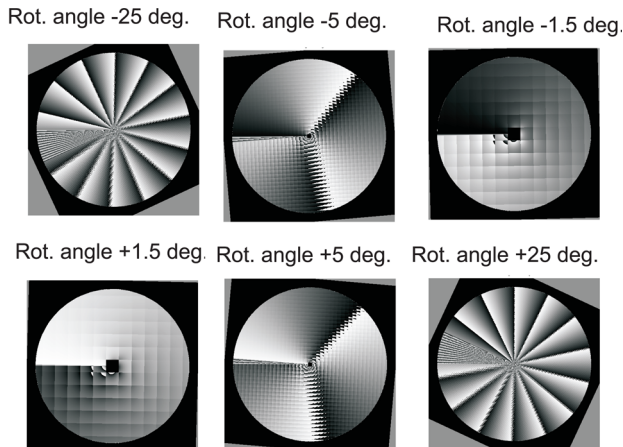


Fig. 11. Combined DOE elements of Fig. 10 at rotation angles of -25° , -5° , -1.5° , $+1.5^\circ$, $+5^\circ$, and $+25^\circ$. The corresponding transmission functions correspond to spiral phase elements with helical indices of approximately -13 , -3 , -1 , $+1$, $+3$, and $+13$, respectively.

in the radially symmetric cases that were treated before, because with this modification, as before, the two spiral phase plates are superposed (instead of being confined to individual sectors), thus giving rise to a second-order moiré effect due to the beating of two helical structures on top of each other, which leads to unwanted effects for some angles.

Nevertheless, Fig. 11 shows that it is possible to design DOE elements according to Eq. (23), with a large a -factor, that generate a considerable change of the helical charge at a rather small mutual rotation angle, such that the area of the undesired sector is sufficiently small for many practical applications, such as the transformation of a Gaussian laser beam into a doughnut mode of an adjustable helical index.

6. Discussion and Conclusions

Combined DOE elements with variable optical properties may have applications in many fields of applied optics, e.g., in cameras, production surveillance systems, laser scanners, beam shapers, fiber optic couplers, or as flexible tools in prototyping and scientific applications. The principle can be down-scaled for, for example, x-ray optical systems, or up-scaled to build large optical components, such as flexible collimation lenses for overhead projectors. The important class of radially symmetric components, such as Fresnel lenses and axicons, has the advantageous feature that the combined MDOE is composed of two identical DOEs, one of them just flipped upside down and placed on top of the other. If the DOEs are properly designed for the desired wavelength, then the obtainable efficiency is close to 100%. For practical applications, optical mounts have to be used that allow the rotation of one element with respect to the other without eccentric displacements. However, even a noncentered DOE pair does not lose its functionality but just acquires lens errors, similar to a misaligned glass lens. Although the principle of combining DOEs to produce new elements has been known for a long time [7], it has not yet led to many practical applications. This might now change, since today industrial methods to produce high-resolution DOEs are readily available. Once a DOE “master” is produced, mass production of cheap copies is possible with embossing methods. Thus, the method may help to produce inexpensive adjustable optical systems.

The authors thank the Austrian Science Fund (project P19582-N20).

References and Notes

1. B. Kress and P. Meyrueis, *Digital Diffractive Optics* (Wiley, 2000).
2. L. B. Lesem, P. M. Hirsch, and J. A. Jordan Jr., “The kinoform: a new wavefront reconstruction device,” *IBM J. Res. Develop.* **13**, 150–155 (1969).
3. R. W. Gerchberg and W. O. Saxton, “A practical algorithm for the determination of phase from image and diffraction plane pictures,” *Optik* **35**, 237–246 (1972).
4. J. M. Burch and D. C. Williams, “Varifocal moiré zone plates for straightness measurement,” *Appl. Opt.* **16**, 2445–2450 (1977).

5. S. Bará, Z. Jaroszewicz, A. Kolodziejczyk, and V. Moreno, "Determination of basic grids for subtractive moiré patterns," *Appl. Opt.* **30**, 1258–1262 (1991).
6. Z. Jaroszewicz, A. Kolodziejczyk, A. Mira, R. Henao, and S. Bará, "Equilateral hyperbolic moiré zone plates with variable focus obtained by rotations," *Opt. Express* **13**, 918–925 (2005).
7. A. W. Lohmann, "A new class of varifocal lenses," *Appl. Opt.* **9**, 1669–1671 (1970).
8. A. Kolodziejczyk and Z. Jaroszewicz, "Diffractive elements of variable optical power and high diffraction efficiency," *Appl. Opt.* **32**, 4317–4322 (1993).
9. In this case $\Phi = ar^2\varphi$, i.e., the first condition, becomes $2ar\varphi < \pi/p$. Considering that $|\varphi|$ can reach the maximal value of π , the condition finally becomes $2ar < 1/p$. On the other hand, the second condition becomes $ar/\pi < 1/p$, which is less restrictive than the first one.
10. S. N. Khonina, V. V. Kotlyar, M. V. Shinkaryev, V. A. Soifer, and G. V. Uspleniev, "The phase rotor filter," *J. Mod. Opt.* **39**, 1147–1154 (1992).
11. N. R. Heckenberg, R. McDuff, C. P. Smith, and A. G. White, "Generation of optical phase singularities by computer-generated holograms," *Opt. Lett.* **17**, 221–223 (1992).
12. N. B. Simpson, D. McGloin, K. Dholakia, L. Allen, and M. J. Padgett, "Optical tweezers with increased axial trapping efficiency," *J. Mod. Opt.* **45**, 1943–1949 (1998).
13. A. Jesacher, S. Fürhapter, S. Bernet, and M. Ritsch-Marte, "Size-selective trapping with optical cogwheel tweezers," *Opt. Express* **12**, 4129–4136 (2004).
14. K. Ladavac and D. G. Grier, "Micro-optomechanical pumps assembled and driven by holographic optical vortex arrays," *Opt. Express* **12**, 1144–1149 (2004).
15. A. Jesacher, S. Fürhapter, C. Maurer, S. Bernet, and M. Ritsch-Marte, "Holographic optical tweezers for object manipulations at an air-liquid interface," *Opt. Express* **14**, 6342–6352 (2006).
16. L. Torner, J. P. Torres, and S. Carrasco, "Digital spiral imaging," *Opt. Express* **13**, 873–881 (2005).
17. J. A. Davis, D. E. McNamara, D. M. Cottrell, and J. Campos, "Image processing with the radial Hilbert transform: theory and experiments," *Opt. Lett.* **25**, 99–101 (2000).
18. C. Maurer, A. Jesacher, S. Fürhapter, S. Bernet, and M. Ritsch-Marte, "Upgrading a microscope with a spiral phase plate," *J. Microsc.* **230**, 134–142 (2008).
19. S. Fürhapter, A. Jesacher, S. Bernet, and M. Ritsch-Marte, "Spiral interferometry," *Opt. Lett.* **30**, 1953–1955 (2005).
20. P. Török and P. R. T. Munro, "The use of Gauss–Laguerre vector beams in STED microscopy," *Opt. Express* **12**, 3605 (2004).